

## Search for the $h_c$ meson in $B^\pm \rightarrow h_c K^\pm$

F. Fang,<sup>5</sup> T. E. Browder,<sup>5</sup> K. Abe,<sup>6</sup> K. Abe,<sup>40</sup> I. Adachi,<sup>6</sup> H. Aihara,<sup>42</sup> D. Anipko,<sup>1</sup>  
 T. Aushev,<sup>11</sup> A. M. Bakich,<sup>37</sup> V. Balagura,<sup>11</sup> M. Barbero,<sup>5</sup> K. Belous,<sup>10</sup> U. Bitenc,<sup>12</sup>  
 I. Bizjak,<sup>12</sup> S. Blyth,<sup>22</sup> A. Bozek,<sup>25</sup> M. Bračko,<sup>6,18,12</sup> A. Chen,<sup>22</sup> W. T. Chen,<sup>22</sup>  
 B. G. Cheon,<sup>3</sup> R. Chistov,<sup>11</sup> Y. Choi,<sup>36</sup> Y. K. Choi,<sup>36</sup> A. Chuvikov,<sup>32</sup> S. Cole,<sup>37</sup>  
 J. Dalseno,<sup>19</sup> M. Danilov,<sup>11</sup> M. Dash,<sup>46</sup> S. Eidelman,<sup>1</sup> S. Fratina,<sup>12</sup> N. Gabyshev,<sup>1</sup>  
 T. Gershon,<sup>6</sup> A. Go,<sup>22</sup> G. Gokhroo,<sup>38</sup> H. Ha,<sup>14</sup> K. Hayasaka,<sup>20</sup> M. Hazumi,<sup>6</sup> D. Heffernan,<sup>29</sup>  
 T. Hokuue,<sup>20</sup> S. Hou,<sup>22</sup> W.-S. Hou,<sup>24</sup> K. Inami,<sup>20</sup> A. Ishikawa,<sup>42</sup> R. Itoh,<sup>6</sup> M. Iwasaki,<sup>42</sup>  
 Y. Iwasaki,<sup>6</sup> J. H. Kang,<sup>47</sup> H. Kawai,<sup>2</sup> T. Kawasaki,<sup>26</sup> H. R. Khan,<sup>43</sup> A. Kibayashi,<sup>43</sup>  
 H. Kichimi,<sup>6</sup> H. J. Kim,<sup>15</sup> K. Kinoshita,<sup>4</sup> P. Križan,<sup>17,12</sup> P. Krokovny,<sup>1</sup> R. Kumar,<sup>30</sup>  
 C. C. Kuo,<sup>22</sup> A. Kuzmin,<sup>1</sup> Y.-J. Kwon,<sup>47</sup> J. Lee,<sup>35</sup> T. Lesiak,<sup>25</sup> S.-W. Lin,<sup>24</sup> D. Liventsev,<sup>11</sup>  
 G. Majumder,<sup>38</sup> F. Mandl,<sup>9</sup> T. Matsumoto,<sup>44</sup> A. Matyja,<sup>25</sup> S. McOnie,<sup>37</sup> W. Mitaroff,<sup>9</sup>  
 K. Miyabayashi,<sup>21</sup> H. Miyake,<sup>29</sup> H. Miyata,<sup>26</sup> Y. Miyazaki,<sup>20</sup> R. Mizuk,<sup>11</sup> D. Mohapatra,<sup>46</sup>  
 E. Nakano,<sup>28</sup> M. Nakao,<sup>6</sup> S. Nishida,<sup>6</sup> O. Nitoh,<sup>45</sup> T. Nozaki,<sup>6</sup> S. Ogawa,<sup>39</sup>  
 T. Ohshima,<sup>20</sup> T. Okabe,<sup>20</sup> S. Okuno,<sup>13</sup> Y. Onuki,<sup>26</sup> H. Ozaki,<sup>6</sup> H. Park,<sup>15</sup> L. S. Peak,<sup>37</sup>  
 R. Pestotnik,<sup>12</sup> L. E. Piilonen,<sup>46</sup> Y. Sakai,<sup>6</sup> T. Schietinger,<sup>16</sup> O. Schneider,<sup>16</sup> R. Seidl,<sup>7,33</sup>  
 K. Senyo,<sup>20</sup> M. E. Sevier,<sup>19</sup> M. Shapkin,<sup>10</sup> H. Shibuya,<sup>39</sup> J. B. Singh,<sup>30</sup> A. Somov,<sup>4</sup>  
 N. Soni,<sup>30</sup> S. Stanič,<sup>27</sup> M. Starič,<sup>12</sup> H. Stoeck,<sup>37</sup> K. Sumisawa,<sup>29</sup> T. Sumiyoshi,<sup>44</sup>  
 F. Takasaki,<sup>6</sup> K. Tamai,<sup>6</sup> M. Tanaka,<sup>6</sup> G. N. Taylor,<sup>19</sup> Y. Teramoto,<sup>28</sup> X. C. Tian,<sup>31</sup>  
 T. Tsukamoto,<sup>6</sup> S. Uehara,<sup>6</sup> T. Uglov,<sup>11</sup> K. Ueno,<sup>24</sup> S. Uno,<sup>6</sup> P. Urquijo,<sup>19</sup> Y. Usov,<sup>1</sup>  
 G. Varner,<sup>5</sup> S. Villa,<sup>16</sup> C. H. Wang,<sup>23</sup> Y. Watanabe,<sup>43</sup> E. Won,<sup>14</sup> B. D. Yabsley,<sup>37</sup>  
 A. Yamaguchi,<sup>41</sup> M. Yamauchi,<sup>6</sup> C. C. Zhang,<sup>8</sup> Z. P. Zhang,<sup>34</sup> and V. Zhilich<sup>1</sup>

(The Belle Collaboration)

<sup>1</sup>*Budker Institute of Nuclear Physics, Novosibirsk*

<sup>2</sup>*Chiba University, Chiba*

<sup>3</sup>*Chonnam National University, Kwangju*

<sup>4</sup>*University of Cincinnati, Cincinnati, Ohio 45221*

<sup>5</sup>*University of Hawaii, Honolulu, Hawaii 96822*

<sup>6</sup>*High Energy Accelerator Research Organization (KEK), Tsukuba*

<sup>7</sup>*University of Illinois at Urbana-Champaign, Urbana, Illinois 61801*

<sup>8</sup>*Institute of High Energy Physics, Chinese Academy of Sciences, Beijing*

<sup>9</sup>*Institute of High Energy Physics, Vienna*

<sup>10</sup>*Institute of High Energy Physics, Protvino*

<sup>11</sup>*Institute for Theoretical and Experimental Physics, Moscow*

<sup>12</sup>*J. Stefan Institute, Ljubljana*

<sup>13</sup>*Kanagawa University, Yokohama*

<sup>14</sup>*Korea University, Seoul*

<sup>15</sup>*Kyungpook National University, Taegu*

<sup>16</sup>*Swiss Federal Institute of Technology of Lausanne, EPFL, Lausanne*

<sup>17</sup>*University of Ljubljana, Ljubljana*

<sup>18</sup>*University of Maribor, Maribor*

<sup>19</sup>*University of Melbourne, Victoria*

- <sup>20</sup>*Nagoya University, Nagoya*  
<sup>21</sup>*Nara Women's University, Nara*  
<sup>22</sup>*National Central University, Chung-li*  
<sup>23</sup>*National United University, Miao Li*  
<sup>24</sup>*Department of Physics, National Taiwan University, Taipei*  
<sup>25</sup>*H. Niewodniczanski Institute of Nuclear Physics, Krakow*  
<sup>26</sup>*Niigata University, Niigata*  
<sup>27</sup>*Nova Gorica Polytechnic, Nova Gorica*  
<sup>28</sup>*Osaka City University, Osaka*  
<sup>29</sup>*Osaka University, Osaka*  
<sup>30</sup>*Panjab University, Chandigarh*  
<sup>31</sup>*Peking University, Beijing*  
<sup>32</sup>*Princeton University, Princeton, New Jersey 08544*  
<sup>33</sup>*RIKEN BNL Research Center, Upton, New York 11973*  
<sup>34</sup>*University of Science and Technology of China, Hefei*  
<sup>35</sup>*Seoul National University, Seoul*  
<sup>36</sup>*Sungkyunkwan University, Suwon*  
<sup>37</sup>*University of Sydney, Sydney NSW*  
<sup>38</sup>*Tata Institute of Fundamental Research, Bombay*  
<sup>39</sup>*Toho University, Funabashi*  
<sup>40</sup>*Tohoku Gakuin University, Tagajo*  
<sup>41</sup>*Tohoku University, Sendai*  
<sup>42</sup>*Department of Physics, University of Tokyo, Tokyo*  
<sup>43</sup>*Tokyo Institute of Technology, Tokyo*  
<sup>44</sup>*Tokyo Metropolitan University, Tokyo*  
<sup>45</sup>*Tokyo University of Agriculture and Technology, Tokyo*  
<sup>46</sup>*Virginia Polytechnic Institute and State University, Blacksburg, Virginia 24061*  
<sup>47</sup>*Yonsei University, Seoul*

## Abstract

We report a search for the  $h_c$  meson via the decay chain  $B^\pm \rightarrow h_c K^\pm$ ,  $h_c \rightarrow \eta_c \gamma$  with  $\eta_c \rightarrow K_S^0 K^\pm \pi^\mp$  and  $p\bar{p}$ . No significant signals are observed. We obtain upper limits on the branching fractions for  $B^\pm \rightarrow \eta_c \gamma K^\pm$  in bins of the  $\eta_c \gamma$  invariant mass. The results are based on an analysis of 253 fb<sup>-1</sup> of data collected by the Belle detector at the KEKB  $e^+e^-$  collider.

PACS numbers: 13.25.Hw, 13.20.-v

The  $h_c$  meson is the  $1^1P_1$  spin singlet state of  $c\bar{c}$ , which is one of the missing states in the charmonium spectrum below  $D\bar{D}$  threshold. It is expected to be a narrow resonance ( $\Gamma_{h_c} < 1.1 \text{ MeV}/c^2$ ) that lies between  $J/\psi(1S)$  and  $\psi(2S)$ . The predicted masses of  $h_c$  vary and are summarized in Ref. [1]. A typical value is less than 10 MeV from the center of gravity of the  $1^3P_J$  states ( $\chi_{c0}$ ,  $\chi_{c1}$  and  $\chi_{c2}$ ), which is  $M_{c.o.g.} = (M_{\chi_{c0}} + 3M_{\chi_{c1}} + 5M_{\chi_{c2}})/9 = 3525.4 \pm 0.1 \text{ MeV}/c^2$ . The  $h_c$  meson should decay dominantly to  $\eta_c\gamma$  with a branching fraction of about 50% [1, 2, 3].

The E760 collaboration has reported an enhancement in the  $p\bar{p} \rightarrow h_c \rightarrow J/\psi\pi^0$  cross section and identified it as the  $1^1P_1$  state with a mass of  $3526.2 \pm 0.25 \text{ MeV}/c^2$  [4]. This result was not confirmed by the subsequent experiment E835 with significantly higher statistics. However, E835[5] reported promising evidence for the  $h_c$  in  $h_c \rightarrow \eta_c\gamma$ . Recently, CLEO[6] has reported the observation of  $h_c \rightarrow \eta_c\gamma$  at a mass of  $M = 3524.4 \pm 0.6 \pm 0.4 \text{ MeV}/c^2$ . The masses obtained by CLEO and E835 are within 1 MeV of  $M_{c.o.g.}$ .

M. Suzuki [3] and others [7] have proposed using the decay chain  $B \rightarrow h_c K$ ,  $h_c \rightarrow \eta_c\gamma$  to look for the  $h_c$  meson. Other charmonium candidates including the  $\eta_c(2S)$ [8],  $X(3872)$ [9] and  $Y(3940)$ [10] were first observed in two-body  $B$  decays, where the kinematic constraints from the exclusive  $B$  decay and production at threshold provide substantial background reduction. The decay amplitudes for  $B \rightarrow h_c K$  and  $B \rightarrow \chi_{c0,2} K$  vanish in the factorization limit. The branching fractions for  $B^+ \rightarrow \chi_{c0,2} K^+$ [11] have been measured and the results are given below [13], [14]:

$$\begin{aligned} \mathcal{B}(B^+ \rightarrow \chi_{c0} K^+) &= (1.34 \pm 0.45 \pm 0.15 \pm 0.04) \times 10^{-4} (\text{BaBar}), \\ \mathcal{B}(B^+ \rightarrow \chi_{c0} K^+) &= (1.12 \pm 0.12 \pm 0.18 \pm 0.08) \times 10^{-4} (\text{Belle}), \\ \mathcal{B}(B^+ \rightarrow \chi_{c2} K^+) &< 0.3 \times 10^{-4}. \end{aligned} \tag{1}$$

The fairly large branching fraction for  $B^+ \rightarrow \chi_{c0} K^+$  suggests that non-factorizable contributions in  $B$  decays to charmonium can be sizable. The decay  $B \rightarrow h_c K$  may occur via the color octet mechanism [15] or re-scattering processes [16] at a rate comparable to that of the factorization allowed decay mode  $B \rightarrow \chi_{c1} K$ . Thus, measurement of the branching fraction for  $B \rightarrow h_c K$  will provide useful information on non-factorizable contributions in  $B$  to charmonium decays.

Here we present the results of a search for  $B^+ \rightarrow h_c K^+$ ,  $h_c \rightarrow \eta_c\gamma$  with  $\eta_c \rightarrow K_S^0 K^\pm \pi^\mp$  and  $p\bar{p}$  using a  $253 \text{ fb}^{-1}$  data sample, which contains  $275 \times 10^6$  produced  $B\bar{B}$  pairs. The data were collected at the  $\Upsilon(4S)$  resonance with the Belle detector at the KEKB  $e^+e^-$  collider[17]. In addition, we use a  $28 \text{ fb}^{-1}$  data sample collected at an energy 60 MeV below resonance to measure the continuum background.

The Belle detector is a large-solid-angle magnetic spectrometer that consists of a silicon vertex detector (SVD), a 50-layer central drift chamber (CDC), an array of aerogel threshold Čerenkov counters (ACC), a barrel-like arrangement of time-of-flight scintillation counters (TOF), and an electromagnetic calorimeter (ECL) comprised of CsI(Tl) crystals located inside a super-conducting solenoid coil that provides a 1.5 T magnetic field. An iron flux-return located outside of the coil is instrumented to detect  $K_L^0$  mesons and to identify muons (KLM). The detector is described in detail elsewhere [18]. A sample of 152 million  $B\bar{B}$  pairs was taken with a 2.0 cm radius beampipe and a 3-layer silicon vertex detector; another sample of 123 million  $B\bar{B}$  pairs was taken with a 1.5 cm radius beampipe, a 4-layer silicon detector and a small-cell inner drift chamber[19].

Event selection criteria were determined using the figure of merit, which is defined as  $S/\sqrt{S+B}$ , where  $B$  is the number of background events and  $S$  is the number of signal events

in a GEANT-based Monte Carlo simulation. We assume  $\mathcal{B}(B^+ \rightarrow h_c K^+) = 3 \times 10^{-4}$  and  $\mathcal{B}(h_c \rightarrow \eta_c \gamma) = 0.5$  for the signal and determine the background  $B$  from the sideband data. Signal events are simulated for five different values of the  $h_c$  mass, which are  $M_{h_c} = 3.23, 3.33, 3.43, 3.527$  and  $3.63 \text{ GeV}/c^2$ , and assuming the intrinsic width  $\Gamma_{h_c} = 1 \text{ MeV}/c^2$ . We determine the final optimization of selection requirements with the  $M_{h_c} = 3.527 \text{ GeV}/c^2$  MC sample.

We select well measured charged tracks with impact parameters with respect to the interaction point (IP) of less than 0.3 cm in the radial direction and less than 5 cm in the  $z$  direction, which is opposite to the positron beam direction. The tracks are required to have the transverse momenta greater than  $50 \text{ MeV}/c$  and have more than 6 axial and 2 stereo CDC hits.

Particle identification likelihoods for the pion and kaon particle hypotheses are calculated by combining information from the TOF and ACC systems with  $dE/dx$  measurements in the CDC. To identify kaons, we require the kaon likelihood ratio,  $L_K/(L_K + L_\pi)$ , to be greater than 0.6, which is 89% efficient for kaons with a 8% misidentification rate for pions. For the charged kaons that come directly from the  $B$  meson rather than from the subsequent decay of the  $\eta_c$ , the kaon likelihood ratio is required to be greater than 0.5. In addition, we remove all kaon candidates that are consistent with being either protons or electrons. To identify pions, we require  $L_K/(L_K + L_\pi)$  to be smaller than 0.7, which is 94% efficient for pions with a 12% misidentification rate for kaons.

Protons and antiprotons are identified using all particle identification systems and are required to have proton likelihood ratios  $[L_p/(L_p + L_K)$  and  $L_p/(L_p + L_\pi)]$  greater than 0.5. Proton candidates that are electron-like according to the information from the ECL are vetoed. This selection is 90% efficient for protons with a 6% misidentification rate for kaons and a 3% misidentification rate for pions.

We select  $K_S^0 \rightarrow \pi^+ \pi^-$  candidates from pairs of oppositely charged tracks that are consistent with the pion hypothesis to form common vertices and lie within the mass window  $0.482 \text{ GeV}/c^2 < M(\pi^+ \pi^-) < 0.514 \text{ GeV}/c^2$ , which corresponds to  $\pm 4\sigma$ . The  $K_S^0$  vertex is required to be displaced from the IP; the vertex direction from the IP is required to be consistent with the  $K_S^0$  flight direction. The  $K_S^0$  requirements are described in detail elsewhere [20].

We reconstruct  $\eta_c$  candidates in the  $K_S^0 K^\pm \pi^\mp$  and  $p\bar{p}$  decay modes. The  $\eta_c$  candidate is required to have an invariant mass in the range between 2.935 and 3.035  $\text{GeV}/c^2$ . In order to reduce the combinatorial background, the charged daughters of the  $\eta_c$  are required to come from a common vertex that is consistent with the interaction point profile.

Photon candidates for the decay  $h_c \rightarrow \eta_c \gamma$  are selected from ECL clusters that are not associated with charged tracks extrapolated from the CDC. We require the photons have energies above 60 MeV, and at least five crystal hits.

To isolate the signal, we form the beam constrained mass  $M_{bc} = \sqrt{E_{\text{beam}}^2 - \vec{P}_{\text{recon}}^2}$  and energy difference  $\Delta E = E_{\text{recon}} - E_{\text{beam}}$ , where  $E_{\text{beam}}$ ,  $E_{\text{recon}}$  and  $\vec{P}_{\text{recon}}$  are the beam energy, the reconstructed energy and the reconstructed momentum of a  $B$  candidate in the  $\Upsilon(4S)$  center of mass frame. The signal region for  $M_{bc}$  is  $5.270 < M_{bc} < 5.290 \text{ GeV}/c^2$ . The signal region for  $\Delta E$  is  $-50 < \Delta E < 35 \text{ MeV}$ , which corresponds to  $\pm 2.5\sigma$  where  $\sigma$  is the resolution determined from a Gaussian fit to the Monte Carlo simulation. If more than one signal candidate is found in an event, we select the one with the largest invariant mass  $M(K^+ \gamma)$ , where the kaon comes from the  $B$ , the best  $\chi^2$  of the  $\eta_c$  vertex and the invariant mass  $M(K_S^0 K^\pm \pi^\mp)$  or  $M(p\bar{p})$  closest to the nominal mass of the  $\eta_c$ . These requirements are imposed in the order listed till only one candidate is selected.

To suppress the large background from continuum  $e^+e^- \rightarrow q\bar{q}$  where  $q = u, d, s, c$ , we first remove events with the normalized second Fox-Wolfram moment  $R_2 > 0.5$ . We then form a likelihood ratio using two variables. Six modified Fox-Wolfram moments[21] and the cosine of the thrust angle are combined into a Fisher discriminant  $\mathcal{F}$ . For signal Monte Carlo and continuum data, we form probability density functions for this Fisher discriminant, and the cosine of the  $B$  decay angle with respect to the  $z$  axis ( $\cos\theta_B$ ). We then calculate the likelihood ratio  $\mathcal{R} = \mathcal{L}_S/(\mathcal{L}_S + \mathcal{L}_{BG})$  for the  $B^+ \rightarrow h_c K^+$  signal Monte Carlo and continuum data. The likelihood ratio  $\mathcal{R}$  for the  $\eta_c \rightarrow K_S^0 K^- \pi^+$  mode is required to be greater than 0.7. This requirement retains 70% of the signal while removing 92% of the continuum background. For the  $p\bar{p}$  mode, which has less continuum background, we require  $\mathcal{R}$  to be greater than 0.6.

In addition to backgrounds from continuum there are also backgrounds from other  $B$  decays. To investigate these backgrounds, we use a sample of  $379 \times 10^6$   $B\bar{B}$  Monte Carlo events. We find that the dominant backgrounds come from  $B^+ \rightarrow \eta_c K^{*+}$ ,  $K^{*+} \rightarrow K^+ \pi^0$  and  $B^0 \rightarrow \eta_c K^{*0}$ ,  $K^{*0} \rightarrow K^+ \pi^-$ . These backgrounds peak in the  $M_{bc}$  distributions. We reject the events if the photon combined with any other photon makes a  $\pi^0$  candidate with  $0.114 < M(\gamma\gamma) < 0.151$  MeV/ $c^2$ . This  $\pi^0$  veto requirement is 83% efficient for signal and removes 51% of background  $\pi^0$ 's. We also require the cosine of the angle in the  $\eta_c\gamma$  rest frame between the  $\gamma$  and the kaon coming from the  $B$  candidate be smaller than 0.6 (0.9) if the invariant mass  $M(\eta_c\gamma)$  is smaller (greater) than 3.5 GeV. These requirements retain 70% (85%) of the signal while removing 67% (72%) of the  $B \rightarrow \eta_c K^*$  backgrounds.

We also find backgrounds from  $B^+ \rightarrow \eta_c K^+$  and  $B \rightarrow D_s^{(*)+} \bar{D}^{(*)}$ , which peak in the  $M_{bc}$  distributions. We remove the  $B^+ \rightarrow \eta_c K^+$  background if the  $\Delta E$  for this decay mode is between  $-60$  and  $+60$  MeV ( $\pm 6\sigma$ ). This requirement is about 100% efficient for the signal. We also apply a  $D_s^+$  veto if the invariant mass  $M(K^+ K_S)$  is in the range  $1.938 < M(K^+ K_S) < 1.998$  GeV/ $c^2$  ( $\pm 3\sigma$ ). This requirement is 94% efficient for the signal.

After all the event selection requirements are applied, no significant peaking  $B\bar{B}$  backgrounds are observed. A component for the  $B\bar{B}$  background is included in the fits to data. In addition, uncertainties in the  $B\bar{B}$  background composition are included in the systematic error.

In Fig. 1, we show the  $M_{bc}$  and  $\Delta E$  distributions in five 100 MeV/ $c^2$  bins of  $M(\eta_c\gamma)$ , which correspond to a  $\pm 3\sigma$  range around the central values used in the signal MC. We determine signal yields from unbinned two-dimensional maximum-likelihood fits to the  $M_{bc}$ - $\Delta E$  distributions in the region  $5.2 < M_{bc} < 5.3$  GeV/ $c^2$  and  $-0.2 < \Delta E < 0.2$  GeV. We use a Gaussian function for  $M_{bc}$  and a double Gaussian for  $\Delta E$  to model the signal. The mean of the Gaussian for  $M_{bc}$  is fixed to 5.279 GeV/ $c^2$ , which is determined from a  $B^+ \rightarrow D^{*0} \pi^+$  data sample, and other parameters are fixed to the values from MC simulation. The functions used to model the backgrounds for other  $B$  decays are determined from MC. The continuum background is modeled with an ARGUS background function that behaves like phase space near the kinematic boundary [22] for  $M_{bc}$  and a linear function for  $\Delta E$ . We determine the shape parameters for the background functions from a fit to the off-resonance data sample. We find that the background shapes do not depend on  $M(\eta_c\gamma)$ . Therefore, we combine the data in the range  $3.17 < M(\eta_c\gamma) < 3.72$  GeV/ $c^2$  to increase statistics.

Because the mass of the  $h_c$  is not well established, we fit the  $M_{bc}$ - $\Delta E$  distributions in the five 100 MeV/ $c^2$  bins of  $M(\eta_c\gamma)$ . The results of the fits are shown in Fig. 1. The signal yields and the detection efficiencies, which are determined from the signal MC samples described above, are given in Table I. No significant signals are observed for  $3.17 < M(\eta_c\gamma) \leq 3.67$

GeV/ $c^2$ .

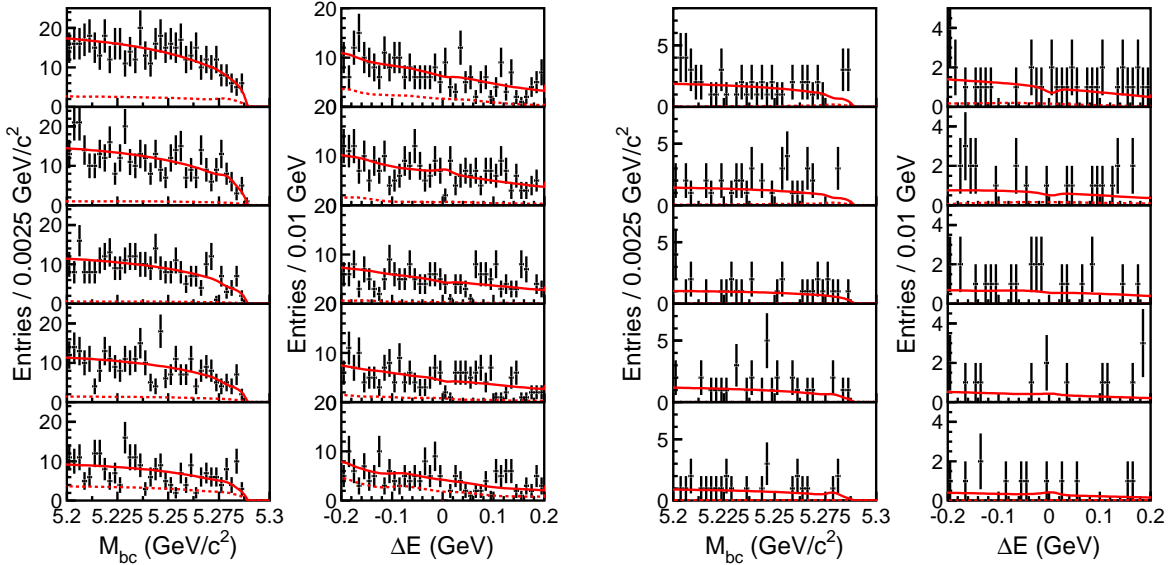


FIG. 1: The  $M_{bc}$  distributions in the  $\Delta E$  signal region and the  $\Delta E$  distributions in the  $M_{bc}$  signal region for the  $\eta_c \rightarrow K_S^0 K^- \pi^+$  (left) and  $\eta_c \rightarrow p\bar{p}$  modes (right) in 100 MeV bins of  $M(\eta_c\gamma)$  for  $3.17 < M(\eta_c\gamma) \leq 3.67$  GeV/ $c^2$ . The distributions are shown in the increasing order of  $M(\eta_c\gamma)$  from the top to the bottom. The solid curves are the results of the fits. The dashed curves represent background components from  $B$  decays.

To check for possible binning effects, we determine the branching fractions for the  $\eta_c\gamma$  invariant mass ranges that are shifted by 50 MeV/ $c^2$  with respect to the nominal range. The results of these fits are shown in Fig. 2. The signal yields and the detection efficiencies are given in Table I. No significant signals are observed for the range  $3.22 < M(\eta_c\gamma) \leq 3.72$  GeV/ $c^2$ .

Fig. 3 shows the  $M(\eta_c\gamma)$  distribution for data in the  $M_{bc}$  and  $\Delta E$  signal region (points with error bars). The distribution is consistent with the background determined from the  $M_{bc}$  sideband data in the region  $5.20 < M_{bc} < 5.26$  GeV/ $c^2$ . The expected contribution for a resonance of a mass of 3.527 GeV/ $c^2$  with a branching fraction at the observed upper limit is also shown.

To demonstrate the effectiveness of the analysis procedure and the method for branching fraction determination, we examine the decay chain  $B^+ \rightarrow \chi_{c1} K^+$ ,  $\chi_{c1} \rightarrow J/\psi\gamma$ ,  $J/\psi \rightarrow p\bar{p}$ . A clear signal of  $14.8_{-3.9}^{+4.6}$  events is observed in the  $M_{bc}$ - $\Delta E$  distribution. We use the yield and the MC detection efficiency of 0.131 to determine the branching fraction  $\mathcal{B}(B^+ \rightarrow \chi_{c1} K^+) = (6.1_{-1.6}^{+1.9}) \times 10^{-4}$ , where the error is statistical only. This is in very good agreement with the result calculated from the world averages [12],  $\mathcal{B}(B^+ \rightarrow \chi_{c1} K^+) = (6.8 \pm 1.2) \times 10^{-4}$ .

The largest contributions to the systematic error in the detection efficiency are the uncertainties in the efficiencies for tracking, particle identification and photon detection. The errors in kaon, pion and proton identification efficiencies are obtained from kinematically selected  $D^{*+} \rightarrow D^0 \pi^+$ ,  $D^0 \rightarrow K^- \pi^+$  and  $\Lambda \rightarrow p \pi^-$  decays in the data. We apply correction factors of 0.975 and 0.941 for the pion and proton detection efficiencies, respectively. The

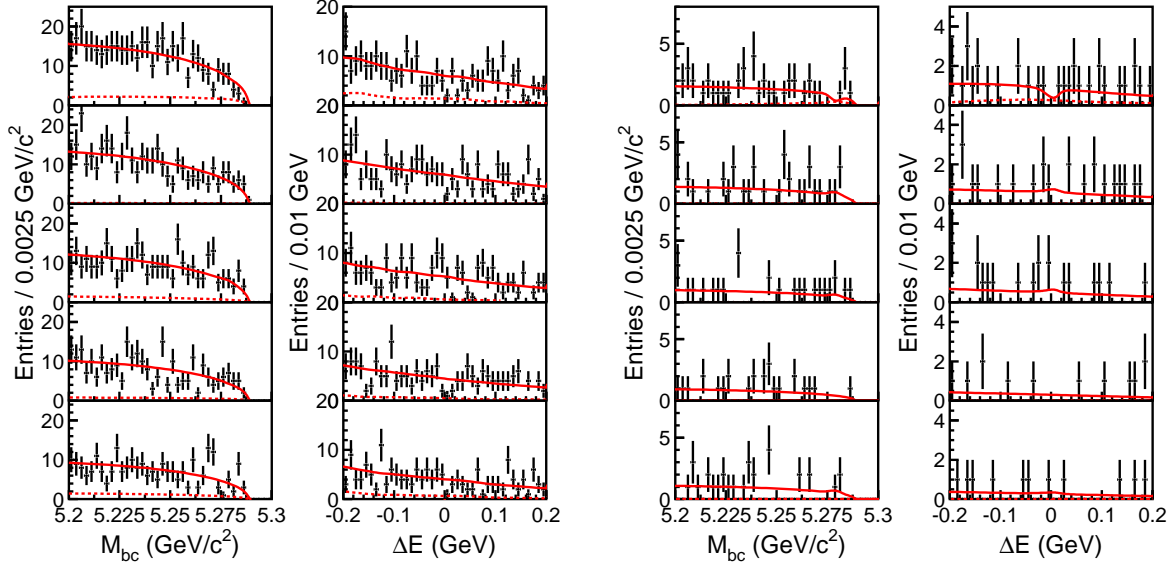


FIG. 2: The  $M_{bc}$  distributions in the  $\Delta E$  signal region and the  $\Delta E$  distributions in the  $M_{bc}$  signal region for the  $\eta_c \rightarrow K_S^0 K^- \pi^+$  (left) and  $\eta_c \rightarrow p \bar{p}$  modes (right) in 100 MeV bins of  $M(\eta_c \gamma)$  for  $3.22 < M(\eta_c \gamma) \leq 3.72$   $\text{GeV}/c^2$ . The distributions are shown in the increasing order of  $M(\eta_c \gamma)$  from the top to the bottom. The solid curves are the results of the fits. The dashed curves represent background components from  $B$  decays.

TABLE I: Detection efficiencies and signal yields in 100  $\text{MeV}/c^2$  bins of  $M(\eta_c \gamma)$ .

$M(\eta_c \gamma)$ ( $\text{GeV}/c^2$ )	$\eta_c \rightarrow K_S^0 K^- \pi^+$		$\eta_c \rightarrow p \bar{p}$	
	$\varepsilon$ (%)	Yield	$\varepsilon$ (%)	Yield
3.17 – 3.27	$4.39 \pm 0.10$	$-3.2^{+5.3}_{-4.3}$	$11.7 \pm 0.2$	$-1.7^{+2.8}_{-2.1}$
3.27 – 3.37	$4.62 \pm 0.10$	$7.0^{+6.0}_{-5.2}$	$12.6 \pm 0.2$	$-1.2^{+1.8}_{-1.3}$
3.37 – 3.47	$5.31 \pm 0.10$	$-3.6^{+3.8}_{-2.7}$	$15.1 \pm 0.2$	$-0.30^{+2.3}_{-1.7}$
3.47 – 3.57	$5.47 \pm 0.10$	$-3.9^{+4.5}_{-3.5}$	$15.1 \pm 0.2$	$-0.76^{+1.9}_{-1.1}$
3.57 – 3.67	$5.95 \pm 0.11$	$3.2^{+5.0}_{-4.3}$	$16.6 \pm 0.2$	$1.4^{+2.0}_{-1.3}$
3.22 – 3.32	$4.66 \pm 0.10$	$-2.2^{+4.9}_{-4.0}$	$12.2 \pm 0.2$	$-3.8^{+2.2}_{-1.8}$
3.32 – 3.42	$4.83 \pm 0.10$	$0.70^{+5.0}_{-4.1}$	$13.8 \pm 0.2$	$1.4^{+2.5}_{-1.8}$
3.42 – 3.52	$5.41 \pm 0.10$	$2.1^{+5.2}_{-4.3}$	$14.9 \pm 0.2$	$1.30^{+2.3}_{-1.5}$
3.52 – 3.62	$5.48 \pm 0.11$	$-1.0^{+4.6}_{-3.8}$	$16.2 \pm 0.2$	$0^{+0.5}_{-0}$
3.62 – 3.72	$6.02 \pm 0.11$	$0.09^{+3.9}_{-3.0}$	$16.9 \pm 0.2$	$1.0^{+2.1}_{-1.4}$

particle identification systematic error is 5.1% for the  $\eta_c \rightarrow K_S^0 K^- \pi^+$  mode and 6.6% for the  $\eta_c \rightarrow p \bar{p}$  mode. The uncertainty in photon detection efficiency is determined to be 5% using a  $\eta \rightarrow \gamma \gamma$  data sample. The uncertainty in the  $\eta_c$  vertex reconstruction is estimated to be 2% using a  $\phi \rightarrow K^+ K^-$  sample. The systematic error due to the modeling of the likelihood ratio cut is determined to be 4% using  $B^+ \rightarrow \bar{D}^0 \pi^+$  events reconstructed in data. We also include the MC statistical uncertainty and the uncertainty in the number of  $B\bar{B}$  pairs in the

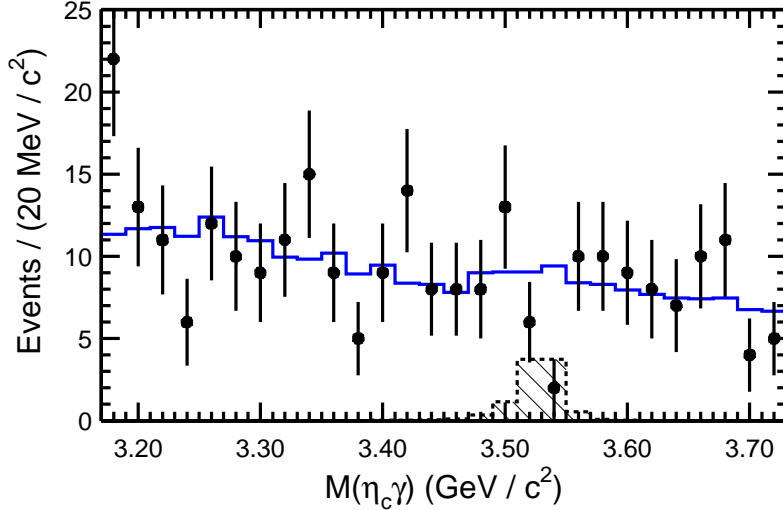


FIG. 3: The  $M(K_S^0 K^\pm \pi^\mp \gamma)$  distributions. The points with error bars are the data in the  $M_{bc}$  and  $\Delta E$  signal region; the solid histogram is the  $M_{bc}$  sideband data in the region  $5.20 < M_{bc} < 5.26$   $\text{GeV}/c^2$ ; the hatched histogram shows the expected contribution for a signal with a branching fraction at the observed upper limit for a resonance with  $M(\eta_c \gamma) = 3.527$   $\text{GeV}$

data sample. The sources of systematic error are combined in quadrature to obtain the final systematic error in the detection efficiency, which is 10.3% for the  $\eta_c \rightarrow K_S^0 K^- \pi^+$  mode and 10.1% for the  $\eta_c \rightarrow p\bar{p}$  mode.

The uncertainty in the signal yield from the fit is determined by varying the mean of the signal for  $M_{bc}$  by  $0.5 \text{ MeV}/c^2$ , and all other shape parameters of the signal and the background by  $1\sigma$  of the measured errors. The results are combined in quadrature to obtain the total uncertainty, which depends on  $M(\eta_c \gamma)$  bin and ranges from  $\pm 0.5$  to  $\pm 2.1$  for the  $\eta_c \rightarrow K_S^0 K^- \pi^+$  mode and from  $\pm 0.0$  to  $\pm 1.3$  for the  $\eta_c \rightarrow p\bar{p}$  mode.

We combine the likelihoods for the  $\eta_c \rightarrow K_S^0 K^- \pi^+$  and  $\eta_c \rightarrow p\bar{p}$  modes, taking into account the respective systematic errors in the detection efficiencies and uncertainties in the signal yields. We determine upper limits at 90% confidence level (C.L.) on the branching fractions for  $B^+ \rightarrow \eta_c \gamma K^+$ . The results are given in Table II in bins of  $M(\eta_c \gamma)$ .

In summary, we have searched for the  $h_c$  meson in the decay chain  $B^+ \rightarrow h_c K^+$ ,  $h_c \rightarrow \eta_c \gamma$ , where the  $\eta_c$  is reconstructed in the  $K_S^0 K^\pm \pi^\mp$  and  $p\bar{p}$  modes. No significant signals are seen for  $3.17 < M(\gamma \eta_c) \leq 3.67 \text{ GeV}/c^2$ . We obtain upper limits on the branching fractions for  $B^+ \rightarrow \gamma \eta_c K^+$  for different  $\eta_c \gamma$  invariant mass ranges. Assuming  $\mathcal{B}(h_c \rightarrow \gamma \eta_c) = 0.5$ , these results give 90% C.L. upper limits on branching fractions for  $B^+ \rightarrow h_c K^+$  as a function of the  $h_c$  mass. The results are shown in Fig. 4. For  $M_{h_c} = 3.527 \text{ GeV}/c^2$ , we find  $\mathcal{B}(B^+ \rightarrow h_c K^+) < 3.8 \times 10^{-5}$ . This is below the lower bound on the  $B \rightarrow h_c K$  branching fraction obtained by Colangelo, Fazio and Pham [16], which is  $\mathcal{B}(B \rightarrow h_c K) = (2 - 12) \times 10^{-4}$ . These results are comparable to the upper limit for  $B^+ \rightarrow \chi_{c2} K^+$  [14] but below the measured rate for  $B^+ \rightarrow \chi_{c0} K^+$ , two other non-factorizable decays. The upper limits obtained in this



TABLE II: Upper limits at 90% C.L. on branching fractions for  $B^+ \rightarrow \gamma\eta_c K^+$  in bins of  $M(\eta_c\gamma)$ .

$M(\eta_c\gamma)$ (GeV/ $c^2$ )	Branching Fraction
3.17 – 3.27	$< 5.9 \times 10^{-5}$
3.27 – 3.37	$< 8.6 \times 10^{-5}$
3.37 – 3.47	$< 3.2 \times 10^{-5}$
3.47 – 3.57	$< 3.8 \times 10^{-5}$
3.57 – 3.67	$< 5.8 \times 10^{-5}$
3.22 – 3.32	$< 4.7 \times 10^{-5}$
3.32 – 3.42	$< 6.7 \times 10^{-5}$
3.42 – 3.52	$< 6.2 \times 10^{-5}$
3.52 – 3.62	$< 2.8 \times 10^{-5}$
3.62 – 3.72	$< 3.9 \times 10^{-5}$

paper assume  $\mathcal{B}(h_c \rightarrow \gamma\eta_c) = 0.5$  and therefore must be renormalized when this  $h_c$  absolute branching fraction is measured. These results may also be used to constrain branching fractions of other charmonium or charmonium-like states that decay to  $\eta_c\gamma$ .

We thank the KEKB group for the excellent operation of the accelerator, the KEK Cryogenics group for the efficient operation of the solenoid, and the KEK computer group and the National Institute of Informatics for valuable computing and Super-SINET network support. We acknowledge support from the Ministry of Education, Culture, Sports, Science, and Technology of Japan and the Japan Society for the Promotion of Science; the Australian Research Council and the Australian Department of Education, Science and Training; the National Science Foundation of China under contract No. 10175071; the Department of Science and Technology of India; the BK21 program of the Ministry of Education of Korea and the CHEP SRC program of the Korea Science and Engineering Foundation; the Polish State Committee for Scientific Research under contract No. 2P03B 01324; the Ministry of Science and Technology of the Russian Federation; the Ministry of Education, Science and Sport of the Republic of Slovenia; the National Science Council and the Ministry of Education of Taiwan; and the U.S. Department of Energy.

- 
- [1] S. Godfrey and J.L. Rosner, Phys. Rev. **D66** 014012 (2002), and references therein.
  - [2] Y.-P. Kuang, S.F. Tuan and T.-M. Yan, Phys. Rev. **D37**, 1210 (1988). P. Ko, Phys. Rev. **D52**, 1710 (1995).
  - [3] M. Suzuki, Phys. Rev. **D66**, 037503 (2002).
  - [4] T.A. Armstrong *et al.* (E760 Collaboration), Phys. Rev. Lett. **69**, 2337 (1992).
  - [5] C. Patrignani *et al.* (E835 Collaboration), contribution to the Proceedings of the BEACH04 conference.
  - [6] J.L. Rosner *et al.*, Phys. Rev. Lett. **95**, 102003 (2005); P. Rubin *et al.*, Phys. Rev. D **72**, 092004 (2005).
  - [7] Y.F. Gu, Phys. Lett. **B 538**, 6 (2002); E. J. Eichten, K. Lane and C. Quigg, Phys. Rev. Lett. **89**, 162002 (2002).
  - [8] S. K. Choi, S. L. Olsen *et al.* (Belle Collaboration), Phys. Rev. Lett. **89**, 102001 (2002).

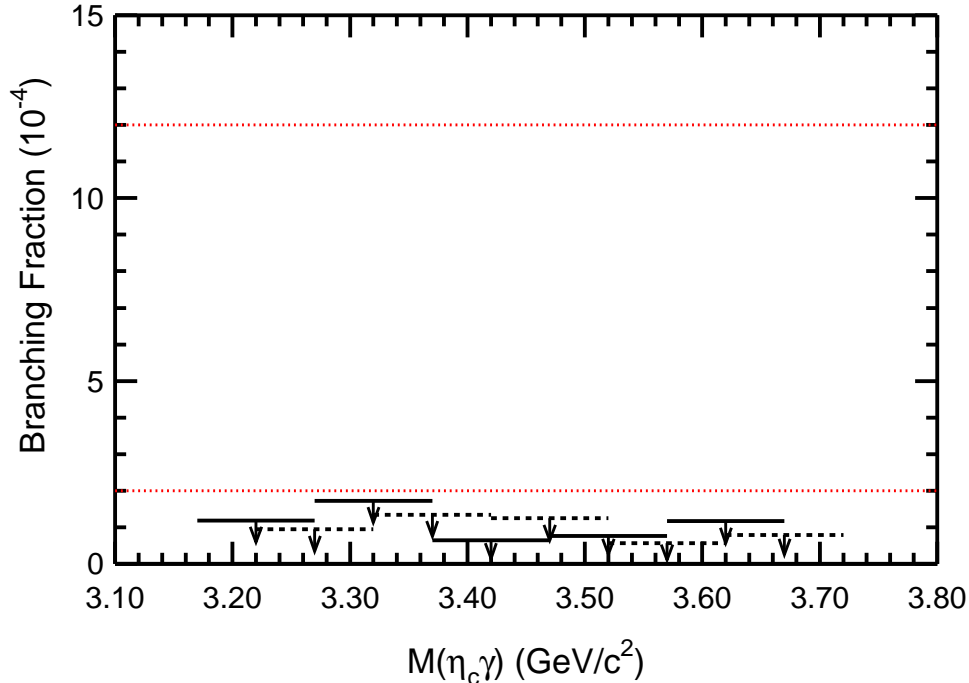


FIG. 4: Upper limits at 90% C.L. on the branching fractions for  $B^+ \rightarrow h_c K^+$  as a function of the  $h_c$  mass, assuming  $\mathcal{B}(h_c \rightarrow \eta_c \gamma) = 0.5$ . The dashed lines with arrows show the upper limits for mass bins shifted by  $50 \text{ MeV}/c^2$  with respect to the nominal ones. The dotted lines represent the theoretical range for the branching fraction obtained by Colangelo, Fazio and Pham [16].

- [9] S. K. Choi, S. L. Olsen *et al.* (Belle Collaboration), Phys. Rev. Lett. 91, 262001 (2003).
- [10] S. K. Choi, S. L. Olsen *et al.* (Belle Collaboration), Phys. Rev. Lett. 94, 182002 (2005).
- [11] The charge conjugate decay mode is implied throughout this paper unless otherwise stated.
- [12] S. Eidelman *et al.*, Phys. Lett. B592, 1 (2004). Also see the 2005 partial year update, where the  $h_c$  is omitted from the summary table and listed as needing confirmation.
- [13] B. Aubert *et al.* (BaBar Collaboration), Phys. Rev. D **72**, 072003 (2005); A. Garmash *et al.* (Belle Collaboration), hep-ex/0512066.
- [14] B. Aubert *et al.* (BaBar Collaboration), Phys. Rev. D **94**, 171801 (2005); N. Soni *et al.* (Belle Collaboration), Phys. Lett. B592, 1 (2004).
- [15] M. Beneke, F. Maltoni and I.Z. Rothstein, Phys. Rev. **D 59**, 054003 (1999).
- [16] P. Colangelo, F. DeFazio and T.N. Pham, Phys. Rev. D **69**, 054023 (2004).
- [17] S. Kurokawa and E. Kikutani, Nucl. Instr. and Meth. A499, 1 (2003), and other papers included in this volume.
- [18] A. Abashian *et al.* (Belle Collab.), Nucl. Instr. and Meth. A **479**, 117 (2002).
- [19] Y. Ushiroda (Belle SVD2 Group), Nucl. Instr. and Meth.A **511** 6 (2003).
- [20] F. Fang, Ph.D thesis, University of Hawaii (2003).

- [21] The Fox-Wolfram moments were introduced in G. Fox and S. Wolfram, *Phys. Rev. Lett.* **41**, 1581 (1978). The modified Fox-Wolfram moments used by Belle are described in M. Nakao *et al.* (Belle Collaboration), *Phys. Rev.* **D 69**, 112001 (2004).
- [22] H. Albrecht *et al.* (ARGUS Collaboration), *Phys. Rev. Lett.* **B241**, 278 (1990).